HHS Public Access

Author manuscript

Biochim Biophys Acta. Author manuscript; available in PMC 2018 July 01.

Published in final edited form as:

Biochim Biophys Acta. 2017 July ; 1859(7): 1273–1281. doi:10.1016/j.bbamem.2017.04.016.

Neuronal excitation and permeabilization by 200-ns pulsed electric field: An optical membrane potential study with FluoVolt dye

Andrei G. Pakhomov[a,*], **Iurii Semenov**[a], **M. Casciola**[a], and **Shu Xiao**[a,b]

[a]Frank Reidy Research Center for Bioelectrics, Old Dominion University, Norfolk, VA, USA

[b]Department of Electrical and Computer Engineering, Old Dominion University, Norfolk, VA, USA

Abstract

Electric field pulses of nano- and picosecond duration are a novel modality for neurostimulation, activation of Ca^{2+} signaling, and tissue ablation. However it is not known how such brief pulses activate voltage-gated ion channels. We studied excitation and electroporation of hippocampal neurons by 200-ns pulsed electric field (nsPEF), by means of time-lapse imaging of the optical membrane potential (OMP) with FluoVolt dye. Electroporation abruptly shifted OMP to a more depolarized level, which was reached within <1 ms. The OMP recovery started rapidly (τ = 8–12 ms) but gradually slowed down (to τ > 10 s), so cells remained above the resting OMP level for at least 20–30 s. Activation of voltage-gated sodium channels (VGSC) enhanced the depolarizing effect of electroporation, resulting in an additional tetrodotoxin-sensitive OMP peak in 4–5 ms after nsPEF. Omitting Ca^{2+} in the extracellular solution did not reduce the depolarization, suggesting no contribution of voltage-gated calcium channels (VGCC). In 40% of neurons, nsPEF triggered a single action potential (AP), with the median threshold of 3 kV/cm (range: 1.9–4 kV/cm); no APs could be evoked by stimuli below the electroporation threshold (1.5–1.9 kV/cm). VGSC opening could already be detected in 0.5 ms after nsPEF, which is too fast to be mediated by the depolarizing effect of electroporation. The overlap of electroporation and AP thresholds does not necessarily reflect the causal relation, but suggests a low potency of nsPEF, as compared to conventional electrostimulation, for VGSC activation and AP induction.

Graphical Abstract

[*]Corresponding author: Andrei G. Pakhomov, Frank Reidy Research Center for Bioelectrics Old Dominion University, 4211 Monarch Way., Suite 300, Norfolk, VA 23508, +1(210)2049012, +1(757)6838003, Fax: +1(757)4511010, 2andrei@pakhomov.net; apakhomo@odu.edu.

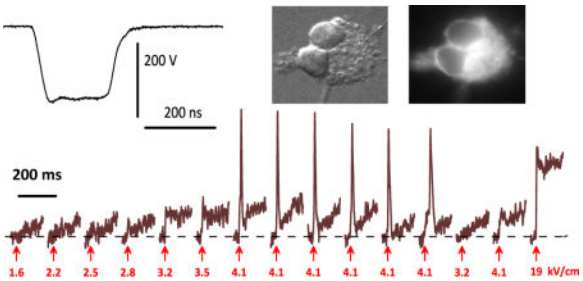

Keywords

Nanosecond pulses; Electroporation; Electropermeabilization; Nanopores; Excitation; Membrane permeability

1. Introduction

Membrane effects of nanosecond pulsed electric fields (nsPEF) have been a subject of steadily increasing attention during the last decade[1–7]. This research has been fueled by exploring the fundamentals of cell membrane biophysics (such as nanopore formation, conduction properties, and resealing), as well as and by emerging nsPEF applications in medicine and biomedical research [1, 8–10].

The formation of permeability pores of nanometer size (“nanopores”) in the cell plasma membrane is arguably the best documented primary effect of nsPEF: It was established by electrophysiological methods[11–14], optical detection of dye and ion uptake[2, 11, 15–18], analysis of cell volume changes[19], as well as by molecular dynamics[20–22] and mathematical modeling[23]. Nanopores display complex conductive properties, including voltage and current sensitivity, inward rectification, and ion selectivity, which have not been fully explained[11, 12, 24]. The formation of nanopores, due to their extraordinary long life span (seconds to minutes) affects practically all aspects of cell physiology, from causing a persistent depolarization of the resting membrane potential (MP)[25, 26], activation of Ca^{2+} [27, 28] and phosphoinositide signaling[3, 29] after a mild permeabilization, to cell volume changes and apoptotic or necrotic cell death[7, 30–32] after more intense treatments.

The reason for nanopore formation is the buildup of transmembrane potential during nsPEF application, up to a high level that causes the disruption of the lipid bilayer. While the membrane in living cells is much more complex than just the bilayer, little is known about nsPEF impact on other membrane constituents. In particular, voltage-gated (VG) ion channels are specifically equipped to detect and respond to MP changes[33], which makes them perhaps the most likely primary target for nsPEF. However, only a handful of studies explored nsPEF effects on VG channels[26, 27, 34–40], with contradictory and uncertain results. This research has been hindered, at least in part, by inherent problems of performing electrophysiological measurements when cells are subjected to intense pulsed electric fields. The amplifier saturation by the electrical pick-up and its unpredictable impact on the command signal in voltage- and current-clamp modes has limited their utility only to delayed effects of nsPEF, and still in combination with non-electrophysiological methods for

additional control[11, 13, 26, 34, 39]. Therefore most studies opted to judge the response of VG calcium and sodium channels (VGCC and VGSC) to nsPEF indirectly, e.g., by optical monitoring of the cytosolic Ca^{2+} after nsPEF, with or without pharmacological channel blockers [28, 34, 35, 37, 40].

In bovine chromaffin cells, Ca^{2+} mobilization by a single 5-ns, 50 kV/cm pulse required opening of L-type VGCC. However the channel opening was not a direct effect of nsPEF, as it depended on the tetrodotoxin-insensitive Na^{+} uptake, possibly due to nanoporation [35]. In adult rat cardiomyocytes, Ca^{2+} mobilization by 4-ns pulses, 10–80 kV/cm, was interpreted as a mixed effect of conventional electrostimulation and the loss of the resting MP due to nanoporation leading to VGCC activation [36]. However, in embryonic rat cardiomyocytes the threshold for eliciting Ca^{2+} transients (36 kV/cm for 10 ns pulses) was lower than the electroporation threshold (63 kV/cm)[40]. In our recent study with 0.5-ns, 190 kV/cm pulses[27], Ca^{2+} mobilization was always mediated by VGCC opening: It was only seen in neurons and neuroblastoma cells (which express VGCC) but not in CHO cells (which do not express VGCC), and the response was sensitive to VGCC blockers. At the same time, cells exposed to nsPEF in a Ca^{2+}-free medium responded to Ca^{2+} when it was added as late as in 10 s after nsPEF, which is probably too long for VGCC to stay open. It was also difficult to explain how VGCC can be opened by pulses which are several orders of magnitude faster than the time needed for translocation of the voltage sensor of the channel[33, 40]. Taken together, these results were indicative of a non-conventional membrane electroporation which involves membrane proteins rather than just lipids [27, 41]. nsPEF exposure could also cause lasting inactivation of both VGCC and VGSC, by an unknown mechanism which apparently did not rely on electroporation[26, 39].

Using whole-cell patch clamp and Ca^{2+} imaging with Fluo-4 (to detect AP-associated Ca^{2+} influx), Cooper and co-authors reported extraordinarily low thresholds for excitation of nociceptor neurons *in vitro* by nsPEF[37]. For 350-ns PEF, the excitation threshold was at 129 V/cm, and could be further reduced in half when applying a 4 kHz pulse train. The membrane integrity was evaluated by the uptake of propidium (Pr). A typical threshold for what was called the “irreversible disruption of the membrane” (defined as >5% increase in Pr fluorescence during the final 30 seconds of a 2-min observation) was at 3–4 kV/cm, i.e., 30–50 times higher than needed for neuroexcitation. The AP threshold with shorter, 12-ns stimuli, was 403 V/cm for single shots, and dropped to measly 16 V/cm for 25-ms long, 4 kHz pulse bursts [34]. These numbers are promising for neurostimulation with nsPEF, but they have not been independently confirmed. The results of Cooper’s group are in stark contrast with other studies which utilized stimuli of comparable duration and reported 20- to 100-fold higher thresholds[24, 27, 28, 35, 36, 38, 40, 42]. Admittedly, all these other studies used endpoints other than AP generation in primary neurons, which could contribute to the inconsistency and emphasized the need to focus exactly on the AP induction in neurons.

The present study centered on the interplay of excitation and permeabilization in rat hippocampal neurons subjected to 200-ns PEF stimuli. Since patch clamp recording might be prone to nsPEF pick-up artifacts, we chose to monitor the optical membrane potential (OMP) using a next generation, fast-responding voltage-sensitive dye FluoVolt (Thermo Fisher Scientific, Waltham, MA). This dye was chosen for its ability to respond to changes

in membrane potential in sub-milliseconds with a high magnitude of emission change. We started with analysis of the dye performance, followed by the comparison of the AP and electroporation thresholds. While no AP could be elicited by nsPEF below the electroporation threshold, the analysis of the fast OMP kinetics suggested that AP could be induced by nsPEF directly and is not necessarily mediated by the electroporation.

2. Materials and Methods

2.1. Cells and media

Dissociated E18 rat hippocampal neurons purchased from BrainBits LLC (Springfield, IL) were seeded on poly-D-lysine/laminin coated glass coverslips (Corning, Corning, NY) in Gibco neurobasal medium supplemented with 50× B-27 (20 ml/l), 100x Glutamax (2.4 ml/l) (all from Thermo Fisher Scientific, Waltham, MA), and 25 μM of L-Glutamic acid (Sigma-Aldrich, St. Louis, MO). One half of the medium was replaced every 3 days, but omitting L-Glutamic acid. Neurons were used between 14 and 30 days in culture.

2.2. Optical membrane potential monitoring with FluoVolt

Loading of cells with the dye and all subsequent manipulations were performed in a Tyrode physiological solution composed of (in mM): 140 NaCl, 5.4 KCl, 2 $CaCl_2$, 1.5 $MgCl_2$, 10 HEPES, and 10 glucose (pH 7.2–7.3, 300–310 mOsm/kg). For 0 Ca^{2+} conditions, $CaCl_2$ was omitted but no Ca^{2+} chelators were used (to prevent their uptake by electropermeabilized cells); the actual free Ca^{2+} level in this solution was 2–5 μM[31]. To make a high-K^+ solution, NaCl was substituted with KCl. All chemicals were from Sigma-Aldrich. In some experiments, VGSC were inhibited with 2 or 4 μM of tetrodotoxin (TTX; Alomone Labs (Jerusalem, Israel).

Cells were loaded with FluoVolt in the physiological solution supplemented with the dye (1:1000x) and with the PowerLoad Concentrate (1:100×), for 15–20 min at room temperature. The PowerLoad Concentrate (a component of the FluoVolt Kit) is an optimized formulation of Pluronic surfactant polyols, which helped the solubilization of the dye. The coverslip was briefly rinsed and placed in a glass-bottomed perfusion chamber (Warner Instruments, Hamden, CT) mounted on a stage of an IX71 microscope (Olympus America, Center Valley, PA). In most experiments, cells were imaged with a PlanApo N 60, 1.42 NA objective (Olympus). The dye was excited from a computer-controlled Sola SE diode light source (Excelitas Technologies Corp., Waltham, MA) using a standard FITC filter cube. Time-lapse images were collected with an iXon Ultra 897 back-illuminated CCD Camera (Andor Technology, Belfast, UK) and Solis interface (Andor). For fast imaging in cropped sensor mode, the camera sensor outside the area of interest was physically shielded with an Optomask (Andor). The light source, the camera, and nsPEF generator were all synchronized and controlled by a TTL pulse protocol using Digidata 1440A board and Clampex v. 10.2 software (Molecular Devices, Sunnyvale, CA). Images were quantified using MetaMorph Advanced v.7.7.0.0 (Molecular Devices, Foster City, CA).

In different sets of experiments, the continuous time lapse image acquisition lasted from less than 200 ms (at 2,325.6 frames/s) to 60 s (at 20 frames/s). For these two examples, a single

nsPEF was delivered, respectively, at precisely 50 ms and 6 s after the onset of imaging. The average emission intensity averaged over a chosen time interval immediately preceding nsPEF (29.7 to 49.8 ms and 5.0–5.95 s, respectively) was taken as 100% (F_0). All frames in the sequence were normalized to this value (F/F_0).

The fluorescence of the background (an area free of any neurites), when measured in specially taken full-frame images, was at about 10% of what was measured over the cell soma. In practice, when we used cropped imaging for higher frame rates, such “empty” areas were impossible to identify. Therefore we did not correct images for the background intensity, with the only possible impact being the reduction of the F/F_0 sensitivity to MP changes by about 10%.

In most series of experiments, the time course of F/F_0 in control (sham-exposed) cells was fit with a polynomial function, and the best fit curve was subtracted to correct for bleaching. However, as shown below, bleaching was much faster in cells severely damaged by nsPEF, resulting in an underestimated correction. The data for multiple independent experiments were averaged and presented as a mean trace with standard error bars. When presenting data for individual cells, the OMP traces were “smoothed” with a running average filter (window = 9 datapoints) to improve visual clarity. Final plots were produced with Grapher 11 software (Golden Software, Golden, CO).

2.3. Nanosecond Pulse Stimulation

Field stimulation and electroporation of individual selected cells on a microscope stage were described in detail previously[2, 17, 18]. To produce nanosecond pulses of a predetermined duration and amplitude, a capacitor of a custom-made generator was fully charged to a desired voltage from a PC-controlled power supply (FJ3R40 Glassman High Voltage, High Bridge, NJ). The capacitor was turned on and off by a power MOSFET switch (IXYS, IXFB38N100Q2) for a given period of time, controlled with a digital delay generator (model 577-8C, Berkeley Nucleonics Corporation, San Rafael, CA). In turn, the delay generator was triggered and synchronized with image acquisitions by a TTL pulse protocol and Clampex software as described above.

The pulses were monitored with a 4 GHz, 20 Gs/s TDS7404 oscilloscope (Tektronix, Beaverton, OR) throughout every experiment. They had trapezoidal shape, with the amplitude at the plateau nearly equal to the charging voltage (Fig. 1A). The rise time increased at higher voltages, and the pulse duration (measured at 50% of the plateau amplitude) decreased from 240 ns at 40 V to less than 180 ns at 600 V (Fig. 1B). In this paper we refer to these pulses as “200-ns long” irrespective of their exact duration or shape.

A pair of tungsten rod electrodes (100 μm diameter, 155 μm gap) was connected to the generator output in parallel to a 50-Ohm load. Using an MPC-200 robotic manipulator (Sutter, Novato, CA), the electrodes were positioned within the microscope field of vision so that the selected cell (or a small group of cells) was centered between the tips of the electrodes (Fig. 1B, inset); then the electrodes were lifted to precisely 50 μm above the coverslip surface.

The electric field at the cell location was determined in a manner similar to what was described previously[2, 18] by 3D numerical simulations using a commercial finite element solver COMSOL Multiphysics, Release 5.0 (COMSOL Inc., Stockholm, Sweden). The electric field values achieved at different charging voltages are presented in Fig. 1B.

3. Results and discussion

3.1. Monitoring neuronal membrane potential with FluoVolt

Our preliminary measurements of OMP with FluoVolt produced conflicting results which were difficult to interpret. This dye has only recently become commercially available, and the few other studies which utilized the dye offered little insight. Therefore it was essential to characterize the response of the dye, to an extent necessary to perform accurate OMP measurements in naïve and electroporated neurons.

A common feature in fluorescent images of neurons loaded with FluoVolt (Fig 2A) is that membranous juxtacellular fibers and formations get stained much brighter than cell bodies. Even if the region of interest is selected strictly over the cell body, the diffuse emission from these structures may “contaminate” the image and result in a lower F/F_0 ratio when the membrane potential changes. This effect could explain why depolarization of neurons with a high-K^+ solution produced, on the average, just a 5% increase in fluorescence (Fig. 2B). Assuming the average resting MP of neurons at −70 mV, the dye sensitivity practically achieved was only about 7% per 100 mV, much less than “up to 20%” expected from the supplier’s description. In addition, even minuscule shifts of cells (by perfusion or by cell swelling after electroporation) could affect the diffuse light contamination and result in erroneous OMP readings. The most stable and higher sensitivity OMP measurements were accomplished when the region of interest was contained within the visible bright perimeter of the cell but did not include it.

With high settings of the excitation light (>30–40% of Sola output) the dye had high phototoxicity and caused 100% cell death within minutes after a 30–60 s illumination (data not shown). Damaged cells “retaliated” by facilitating dye bleaching (possibly by releasing ROS) far beyond the bleaching rate in intact cells, the effect which could be misinterpreted for hyperpolarization (see Section 3.2). Fortunately, the phototoxicity was not noticeable at low light settings (<10% of Sola output) and in practice less than 5% of the light output was adequate even for the fastest imaging.

With a low-light illumination, the FluoVolt emission showed complex time dynamics, which is collectively regarded here as “bleaching”, although the process appears far more complex (Fig. 2C). For a 1-min long, 20 frames/s recording, the emission dropped sharply during the first 3–4 s; then the reduction slowed down or even temporarily reversed in some cells (from 5 to 20–30 s), followed by a faster and almost linear decline for the rest of the acquisition time. When nsPEF stimuli were applied (next section), this was done at 6 s into the recording (arrow), to avoid the initial steep decline. The best fit shown by a dashed line in Fig. 2C could only be accomplished by a 9^{th} degree polynomial function; such complex time dynamics indicates that the dye emission is impacted by diverse concurrent processes (their detailed analysis was beyond the scope of this work). Of note, the CCD camera performance

during time lapse acquisitions was not one of these processes; when the fluorescence signal was substituted by a similar intensity illumination from a battery-operated diode flashlight, the measured signal was stable.

On a much faster time scale (200 ms total, 2325.6 frames/s, Fig. 2D), bleaching started very fast (by 0.5–1% in 10–15 ms), then slowed down and became nearly linear. The best fit shown in Fig 2D disregards the initial steep decline segment and has been accomplished by a 4^{th} degree polynomial function. In experiments with nsPEF, the stimulus was delivered at 50 ms, whereas the emission measurements for the first 10 or 20 ms were discarded.

When the excitation light was turned off, the dye gradually recovered from bleaching. When immediate effects of nsPEF were probed by a fast imaging protocol (such as in Fig. 2D) in the same cell repeatedly with 1-min “dark” intervals, the starting emission level did not necessarily reflect the actual de- or repolarization of the cell membrane during this 1-min rest. Thus the slow and fast OMP measurements after nsPEF could only be accomplished in separate experiments.

When taking the above caveats into account, the FluoVolt dye has proven accurate and reliable; it was indispensable for fast OMP recording with high-amplitude nsPEF stimuli, instead of EMF interference-prone electrophysiological methods.

3.2. Electroporation by nsPEF and the time course of OMP recovery

Persistent loss of the resting MP for tens of seconds and minutes is a well-known manifestation of cell membrane permeabilization (electroporation) by nsPEF[24, 25], but the time course of the depolarization and MP recovery have not been studied.

MP depolarization by opening of endogenous VGCC and VGSC, by any stimulus, is not expected to last more than tens or hundreds of milliseconds; in contrast, depolarization of the resting MP for tens of seconds after nsPEF was a sign of electroporative membrane permeabilization. A single pulse at 1.5 kV/cm caused no effect in most cells, but at 3.1 kV/cm and higher it caused abrupt depolarization which lasted 20–30 s or longer (Fig. 3A). The restoration towards the initial resting MP started rapidly but slowed down, reaching a plateau slightly above the initial level (3.1 and 6.2 kV/cm). Paradoxically, the MP recovery (judged as a decrease in dye emission) after still more intense pulses (Fig. 3A, 12.6 and 18.2 kV/cm) appeared as a faster process. In actuality, this reduction of dye emission occurred for reasons unrelated to hyperpolarization, perhaps because of bleaching by reactive oxygen species released in cells severely damaged by nsPEF[43, 44].

Indeed, applying multiple nsPEF (10 pulses with 4 s intervals) demonstrated that OMP hyperpolarization was an artifact. The second and subsequent pulses in the train caused gradually weakening responses, consistent with an already depolarized state, when an additional permeabilization cannot depolarize the MP any further (Fig. 3B). In contrast, the emission steadily decreased, and the decrease was steeper in cells subjected to most intense pulses (i.e., most damaged). The cell damage was also easily recognizable by visual inspection as a loss of differential interference contrast and “volume” in cells subjected to

multiple intense pulses (data not shown). Such morphological changes are characteristic for complete membrane rupture and permanent MP loss.

Overall, FluoVolt dye was a reliable indicator of the depolarization caused by nsPEF, whereas its utility for monitoring the MP recovery was somewhat limited. We can nonetheless state that the MP recovery took a minimum of 20–30 s, since a proper correction for bleaching would only make these numbers larger.

The early kinetics of repolarization can be better appreciated from Fig. 4. Panel A shows the data from Fig. 3A brought together in a single plot and on a faster time scale, and panel B shows data from an independent set of experiments with a shorter exposure time and higher frame rate. The gradually decreasing rate of the repolarization can be quantified by the increase of the time constant for the best exponential fit with the time after nsPEF application: from 8–10 ms immediately after nsPEF (see Section 3.4), to 40–50 ms within 0.2–0.3 s, 1.5–2 s within 6–8 s, and 10–16 s in the interval 15–40 s after nsPEF (the numbers are from fitting data for 2.5, 3.1, and 6.2 kV/cm in Figs 3A, and 4A and B; best fits are not shown for clarity). Such data indicate the involvement of several different repolarization mechanisms, including the activation and inactivation of endogenous VG channels, which could contribute to the brief depolarization peak revealed in Fig. 4B early after nsPEF. This peak explains the larger values of the maximum depolarization when it was measured at the faster frame rate and using shorter exposure (Fig. 4C), whereas with longer exposures it was leveled out. The nsPEF effect in both sets of experiments reached saturation at about 5% emission increase, which also matched value for perfusion with a high-K+ solution. The expected OMP “overshoot” from nsPEF-induced APs was probably offset by averaging across cells which did and did not fire AP. *3.3 Triggering action potentials by 200-ns stimuli*

3.3 Triggering action potentials by 200-ns stimuli

Above we showed that the threshold for electroporation by a single 200-ns pulse, as evidenced by persistent OMP depolarization, was at 1.5–2 kV/cm (Fig. 4C). If APs can be elicited by nsPEF intensities below this threshold, this would prove that nsPEF can activate VGSC directly, without electroporation-induced depolarization as an intermediate step.

We used fast imaging (0.43 ms exposure time, 2325.6 frames/s) to capture APs and analyze the fast kinetics of OMP change. A single nsPEF was applied exactly at 50 ms after the onset of image acquisition. Each time-lapse stack included 450 frames and lasted 193 ms, to minimize possible phototoxic effects while allowing to capture APs and depolarization due to electroporation. Such time lapse imaging series were repeated multiple times in each neuron automatically, always with a 60-s interval which allowed for saving the data and changing the nsPEF amplitude, if needed.

All measurements were performed with a single cell at a time and started by applying a pulse at 1.3 kV/cm, the intensity just below the electroporation threshold. Should a neuron respond with an AP, the pulse amplitude would be decreased in the next trials, until the AP threshold was reached. However, in case of no response to 1.3 kV/cm, the pulse amplitude would be increased, to test if the cell would fire APs concurrently with electroporation. If a

cell never generated APs and also did not respond to intense nsPEF at the end of the experiment with depolarization, it was regarded non-viable and excluded from analyses.

These experiments established that cells never responded to 1.3 kV/cm pulses; hence the pulse amplitude always had to be tuned up from the first trial. Because of the lack of responses, eventually we increased the starting amplitude to 1.6–1.9 kV/cm. Out of 57 cells tested and proven viable, nsPEF induced APs in 23 neurons (40%), but only at amplitudes at or above the electroporation threshold. OMP traces if four representative cells (Fig. 5, A–D) show AP thresholds at 2.5 kV/cm or higher. The mean AP threshold was about 3 kV/cm (Fig. 5E), well above the established electroporation threshold as measured from data in Figs. 3 and 4. In some but not all cells, electroporation could be clearly observed before any APs were elicited (Fig. 5C) and was also seen as persistent depolarization after the AP (Fig. 5C,D).

Repeated nsPEF evoked APs of gradually diminishing amplitude and eventually became ineffective; further increase in nsPEF amplitude did not restore firing. Such “fatigue” could result from repeated cell damage by nsPEF, but could also be caused by the dye phototoxicity. Bath addition of tetrodotoxin abolished firing (Fig. 5B), confirming that the recorded fast OMP peaks are indeed APs caused by VGSC activation.

3.4. Role of endogenous ion channels in the depolarization response to nsPEF

In the next set of experiments, the nsPEF stimulation and OMP monitoring protocols were kept the same for all cells. Only one experiment was performed in each cell, and only one cell was imaged in each experiment. The selected cell was stimulated six times with 1-min intervals, with the pulse amplitude being increased, in several steps, from 1.9 in the first trial to 18 kV/cm in the last one (as in Fig. 5D). OMP was imaged at 2325.6 frames/s, starting 50 ms before each stimulus and ending 143 ms after it; thus each experiment yielded 6 stacks of 450 images each.

The experiments were performed in (1) standard Tyrode solution, (2) the same solution without added $CaCl_2$ (“0 Ca^{2+}”), (3) standard Tyrode solution with 4 μM TTX, or (4) 0 Ca^{2+} solution with 4 μM TTX. Comparing these different conditions was aimed at identifying the role of VGCC and VGSC in the MP changes evoked by nsPEF and separating thresholds for excitation and electroporation.

In the standard Tyrode solution, 1.9 kV/cm nsPEF elicited no response. At 2.5 kV/cm and higher, it caused depolarization which started with a brief peak (10–20 ms) followed by a plateau at still depolarized OMP (Fig 6A). The transition from the peak to the plateau could be fit with a single exponential function with τ = 8–12 ms. This initial peak but not the plateau was abolished by TTX (Fig. 6C, with the exception of 18 kV/cm), proving that the peak results from VGSC opening. The amplitude and duration of this peak matched those of an AP, whereas its relatively small amplitude was a result of data averaging for cells which did not fire AP, and for cells which fired APs with somewhat different latency after nsPEF. The plateau level increased only marginally when nsPEF was escalated from 3.1 to 4.7 kV/cm, because of incomplete resting MP recovery during 1-min rest after the previous stimulus.

The removal of Ca^{2+} had no apparent impact on the response shape, although its amplitude slightly increased (Fig. 6B). One neuron (out of 11) fired an AP after a 1.9 kV/cm pulse, with no concurrent manifestations of electroporation (although they could be concealed by the noise). VGCC opening did not contribute to OMP depolarization by nsPEF, whereas the reduction of the ambient Ca^{2+} could slightly increase the sensitivity to nsPEF. The addition of TTX to 0 Ca^{2+} solution had the same effect as in normal Tyrode (inhibition of the first peak of depolarization), along with slight increase of the depolarization amplitude (Fig. 6D).

The data in Fig 6 confirm that the fast, sustained depolarization in response to nsPEF does not depend on the activation of VGSC or VGCC. The depolarization response in the presence of TTX and in the absence of Ca^{2+} is a result of a leak current through electropores (although it is not easy to distinguish between “true” lipid pores and some non-VG ion channels; see [11] for discussion). The change in OMP due to electroporation was extremely fast: the maximum depolarization (appearing as a plateau with fast recording in Figs. 6 and 7) was already achieved by the second image taken after nsPEF, i.e., in less than 1 ms (Fig. 7). The rate of OMP change (1–2% per 1 ms, equivalent to 15–30 V/s) was comparable to that of an nsPEF-induced AP, but the peak of AP was reached later, only in about 4 ms. In the first approximation, the current carried through nanopores was comparable to the VGSC current during the rising phase of AP. The abrupt transition from the fast OMP change to the plateau after 18 kV/cm nsPEF simply suggests that the OMP has hit zero potential. However, the same abrupt transition after 3.1 kV/cm nsPEF, with the OMP leveling far before reaching zero potential, is intriguing and may unveil important quantitative details about pore formation, and properties. First, this transition may be a manifestation of two distinct steps in the early pore evolution, which has long been suspected but never demonstrated by a direct experiment. It was a stark contrast between the pore lifetime in molecular dynamics simulations[45, 46] and in experimental measurements of membrane conductance[11–13, 25, 47] that has led to a hypothesis that many short-lived pores form during the pulse but only a few of them are modified to survive for minutes. Pores may get stabilized by obstruction with macromolecules[48, 49], or may form long-lived membrane permeability structures[50]. A two-step process of membrane permeabilization was also considered as a mechanism of bipolar cancellation effect[47, 51]. Second, the plateau level is a new equilibrium potential, which is determined by (a) the permeabilities of endogenous ion channels and electropores, and (b) by transmembrane ion gradients. For future studies, measuring the plateau level while varying the ionic composition of the medium will provide valuable data on the conductivity, size, and ion selectivity of electropores.

4. Conclusions

This study, for the first time, employed fast OMP imaging to analyze the neuronal excitation and electroporation by 200-ns PEF, on different time scales. OMP imaging is free of electrical pick-up artifacts which are inherent for electrophysiological methods and limit their utility in studies with nsPEF. We found that electroporation causes rapid membrane depolarization (within < 1 ms), which, however, may stop before hitting zero transmembrane potential. The re-polarization to the resting MP starts as a rapid process (τ = 8–12 ms) but gradually slows down (to τ > 10s) and takes tens of seconds. VGCC did not contribute to

OMP depolarization, whereas opening of VGSC could lead to the generation of a single AP that peaked at 4–6 ms after nsPEF.

Electroporation occurred consistently at nsPEF amplitudes of 1.5–3 kV/cm and higher. The principal finding of this study is that APs could only be evoked by nsPEF at or above the electroporation threshold, which contrasts a large gap between stimulation and electroporation thresholds for micro- and millisecond duration pulses. While such data suggest a causal connection (electroporation causes depolarization, which activates VGSC to fire an AP), such connection cannot be proven without selectively blocking electroporation and testing if this would prevent AP firing. However, the only known blockers of electropores (Gd^{3+} and La^{3+}[18, 52]) are also potent inhibitors of diverse ion channels, and may block AP on their own.

With conventional stimuli (e.g., 100 μs to 10 ms long), regardless of their amplitude, the build-up of the transmembrane potential proceeds relatively slowly, by means of ionic (Maxwell-Wagner) polarization. This process allows enough time for VG channels to respond; opening of these channels alleviates or prevents further build-up of the transmembrane potential, thus protecting cells from the electroporative damage. However, opening of VGSC is not instantaneous; it involves physical translocation of the voltage sensor of the channel within the membrane, which takes on the order of 10–100 μs[33]. This mechanism is too slow to render any protection from 200-ns pulses by decelerating the transmembrane potential buildup. The lack of such protection will expectedly narrow the gap between stimulating and porating thresholds.

At the same time, the data in Fig. 7 show that VGSC activation occurred very early, and contributed to depolarization already at the first timepoint (<0.5 ms) after nsPEF (the contribution of VGSC is the difference between responses to 3.1 kV/cm with and without TTX). At this time, the change in OMP due to electroporation reached only 0.4% (approx. 6 mV), which is too small to activate VGSC. In just a few experiments, the AP emerged with a larger delay after nsPEF and probably was a result of electroporation (averaging such “late” and “early” APs caused broadening of the averaged AP peak in Fig. 6A, 3.8 kV/cm). However, in most neurons, VGSC activation occurred early and was likely a direct effect of nsPEF, not mediated by electroporation-induced depolarization. This conjecture is further supported by (1) occurrences of AP without concurrent manifestations of electroporation (such in Fig. 5A, B), (2) our earlier data that compared excitation and poration in embryonic cardiomyocytes[40], and (3) our recent findings that 10-ns PEF can stimulate isolated sciatic nerve, generating thousands of APs without electroporative damage (unpublished).

Thus we conclude that nsPEF has relatively low potency for electrostimulation as compared to electroporation, and the overlap of the respective thresholds is a result of narrowing the gap between them, rather than a reflection of a causal connection. We were unable to support the reports by Cooper’s group about excitation of neurons at only 129 V/cm for nsPEF of comparable duration, 350 ns[37]. However, the electroporation threshold established in their study by the Pr uptake assay, 3–4 kV/cm, was not much different from our data, when taking into account low sensitivity of this assay for nanopore detection[2, 11, 17].

Acknowledgments

The study was supported by R21EB016912 from NIBIB (to SX and AGP) and by an AFOSR MURI grant FA9550-15-1-0517 (to AGP) on Nanoelectropulse-Induced Electromechanical Signaling and Control of Biological Systems, administered through Old Dominion University.

Abbreviations

AP	action potential
MP	membrane potential
OMP	optical membrane potential
nsPEF	nanosecond pulsed electric field
TTX	tetrodotoxin
VGCC	voltage-gated calcium channel
VGSC	voltage-gated sodium channel

References

1. Schoenbach KS, Hargrave B, Joshi RP, Kolb J, Osgood C, Nuccitelli R, Pakhomov AG, Swanson J, Stacey M, White JA, Xiao S, Zhang J, Beebe SJ, Blackmore PF, Buescher ES. Bioelectric Effects of Nanosecond Pulses. IEEE Transactions on Dielectrics and Electrical Insulation. 2007; 14:1088–1109.
2. Pakhomov AG, Gianulis E, Vernier PT, Semenov I, Xiao S, Pakhomova ON. Multiple nanosecond electric pulses increase the number but not the size of long-lived nanopores in the cell membrane. Biochim Biophys Acta. 2015; 1848:958–966. [PubMed: 25585279]
3. Tolstykh GP, Beier HT, Roth CC, Thompson GL, Ibey BL. 600ns pulse electric field-induced phosphatidylinositol-bisphosphate depletion. Bioelectrochemistry. 2014; 100:80–87. [PubMed: 24530104]
4. Pakhomov, AG., Miklavcic, D., Markov, MS. Advanced Electroporation Techniques in Biology in Medicine. CRC Press: Boca Raton: 2010. p. 528
5. Roth CC, Tolstykh GP, Payne JA, Kuipers MA, Thompson GL, DeSilva MN, Ibey BL. Nanosecond pulsed electric field thresholds for nanopore formation in neural cells. Journal of biomedical optics. 2013; 18:035005. [PubMed: 23532338]
6. Napotnik TB, Wu YH, Gundersen MA, Miklavcic D, Vernier PT. Nanosecond electric pulses cause mitochondrial membrane permeabilization in Jurkat cells. Bioelectromagnetics. 2012; 33:257–264. [PubMed: 21953203]
7. Morotomi-Yano K, Akiyama H, Yano K. Nanosecond pulsed electric fields induce poly(ADP-ribose) formation and non-apoptotic cell death in HeLa S3 cells. Biochem Biophys Res Commun. 2013; 438:557–562. [PubMed: 23899527]
8. Nuccitelli R, Huynh J, Lui K, Wood R, Kreis M, Athos B, Nuccitelli P. Nanoelectroablation of human pancreatic carcinoma in a murine xenograft model without recurrence. Int J Cancer. 2013; 132:1933–1939. [PubMed: 23001643]
9. Nuccitelli R, Berridge JC, Mallon Z, Kreis M, Athos B, Nuccitelli P. Nanoelectroablation of Murine Tumors Triggers a CD8-Dependent Inhibition of Secondary Tumor Growth. PLoS One. 2015; 10:e0134364. [PubMed: 26231031]
10. Breton M, Mir LM. Microsecond and nanosecond electric pulses in cancer treatments. Bioelectromagnetics. 2012; 33:106–123. [PubMed: 21812011]

11. Pakhomov, AG., Pakhomova, ON. Nanopores: A distinct transmembrane passageway in electroporated cells. In: Pakhomov, AG.Miklavcic, D., Markov, MS., editors. Advanced Electroporation Techniques in Biology in Medicine. CRC Press; 2010. p. 178-194.Place Published
12. Ibey BL, Mixon DG, Payne JA, Bowman A, Sickendick K, Wilmink GJ, Roach WP, Pakhomov AG. Plasma membrane permeabilization by trains of ultrashort electric pulses. Bioelectrochemistry. 2010; 79:114–121. [PubMed: 20171148]
13. Pakhomov AG, Bowman AM, Ibey BL, Andre FM, Pakhomova ON, Schoenbach KH. Lipid nanopores can form a stable, ion channel-like conduction pathway in cell membrane. Biochem Biophys Res Commun. 2009; 385:181–186. [PubMed: 19450553]
14. Pakhomov AG, Shevin R, White JA, Kolb JF, Pakhomova ON, Joshi RP, Schoenbach KH. Membrane permeabilization and cell damage by ultrashort electric field shocks. Arch Biochem Biophys. 2007; 465:109–118. [PubMed: 17555703]
15. Vernier PT, Sun Y, Gundersen MA. Nanoelectropulse-driven membrane perturbation and small molecule permeabilization. BMC Cell Biol. 2006; 7:37. [PubMed: 17052354]
16. Vernier PT, Sun Y, Chen MT, Gundersen MA, Craviso GL. Nanosecond electric pulse-induced calcium entry into chromaffin cells. Bioelectrochemistry. 2008; 73:1–4. [PubMed: 18407807]
17. Bowman AM, Nesin OM, Pakhomova ON, Pakhomov AG. Analysis of plasma membrane integrity by fluorescent detection of Tl(+) uptake. J Membr Biol. 2010; 236:15–26. [PubMed: 20623351]
18. Gianulis EC, Pakhomov AG. Gadolinium modifies the cell membrane to inhibit permeabilization by nanosecond electric pulses. Arch Biochem Biophys. 2015; 570:1–7. [PubMed: 25707556]
19. Nesin OM, Pakhomova ON, Xiao S, Pakhomov AG. Manipulation of cell volume and membrane pore comparison following single cell permeabilization with 60- and 600-ns electric pulses. Biochim Biophys Acta. 2011; 3:792–801.
20. Ho MC, Casciola M, Levine ZA, Vernier PT. Molecular Dynamics Simulations of Ion Conductance in Field-Stabilized Nanoscale Lipid Electropores. J Phys Chem B. 2013; 117:11633–11640. [PubMed: 24001115]
21. Casciola M, Bonhenry D, Liberti M, Apollonio F, Tarek M. A molecular dynamic study of cholesterol rich lipid membranes: comparison of electroporation protocols. Bioelectrochemistry. 2014; 100:11–17. [PubMed: 24731593]
22. Casciola M, Tarek M. A molecular insight into the electro-transfer of small molecules through electropores driven by electric fields. Biochim Biophys Acta. 2016; 1858:2278–2289. [PubMed: 27018309]
23. Son RS, Smith KC, Gowrishankar TR, Vernier PT, Weaver JC. Basic Features of a Cell Electroporation Model: Illustrative Behavior for Two Very Different Pulses. J Membr Biol. 2014
24. Semenov I, Xiao S, Pakhomov AG. Electroporation by subnanosecond pulses. Biochemistry and biophysics reports. 2016; 6:253–259. [PubMed: 27482547]
25. Pakhomov AG, Kolb JF, White JA, Joshi RP, Xiao S, Schoenbach KH. Long-lasting plasma membrane permeabilization in mammalian cells by nanosecond pulsed electric field (nsPEF). Bioelectromagnetics. 2007; 28:655–663. [PubMed: 17654532]
26. Nesin V, Bowman AM, Xiao S, Pakhomov AG. Cell permeabilization and inhibition of voltage-gated Ca(2+) and Na(+) channel currents by nanosecond pulsed electric field. Bioelectromagnetics. 2012; 33:394–404. [PubMed: 22213081]
27. Semenov I, Xiao S, Kang D, Schoenbach KH, Pakhomov AG. Cell stimulation and calcium mobilization by picosecond electric pulses. Bioelectrochemistry. 2015; 105:65–71. [PubMed: 26011130]
28. Craviso GL, Choe S, Chatterjee I, Vernier PT. Modulation of intracellular Ca(2+) levels in chromaffin cells by nanoelectropulses. Bioelectrochemistry. 2012; 87:244–252. [PubMed: 22197468]
29. Tolstykh GP, Tarango M, Roth CC, Ibey BL. Nanosecond pulsed electric field induced dose dependent phosphatidylinositol-4,5-bisphosphate signaling and intracellular electro-sensitization. Biochim Biophys Acta. 2017; 1859:438–445. [PubMed: 28064021]
30. Muratori C, Pakhomov AG, Gianulis EC, Jensen SD, Pakhomova ON. The cytotoxic synergy of nanosecond electric pulses and low temperature leads to apoptosis. Sci Rep. 2016; 6:36835. [PubMed: 27833151]

31. Pakhomova ON, Gregory B, Semenov I, Pakhomov AG. Calcium-mediated pore expansion and cell death following nanoelectroporation. Biochim Biophys Acta. 2014; 1838:2547–2554. [PubMed: 24978108]
32. Ren W, Beebe SJ. An apoptosis targeted stimulus with nanosecond pulsed electric fields (nsPEFs) in E4 squamous cell carcinoma. Apoptosis. 2011; 16:382–393. [PubMed: 21213047]
33. Hille, B. Ionic Channels of Excitable Membranes. 3. Sinauer Associates; 2001. Place Published
34. Jiang N, Cooper BY. Frequency-dependent interaction of ultrashort E-fields with nociceptor membranes and proteins. Bioelectromagnetics. 2011; 32:148–163. [PubMed: 21225892]
35. Craviso GL, Choe S, Chatterjee P, Chatterjee I, Vernier PT. Nanosecond electric pulses: a novel stimulus for triggering Ca2+ influx into chromaffin cells via voltage-gated Ca2+ channels. Cell Mol Neurobiol. 2010; 30:1259–1265. [PubMed: 21080060]
36. Wang S, Chen J, Chen MT, Vernier PT, Gundersen MA, Valderrabano M. Cardiac myocyte excitation by ultrashort high-field pulses. Biophysical journal. 2009; 96:1640–1648. [PubMed: 19217879]
37. Nene D, Jiang N, Rau KK, Richardson M, Cooper BY. Nociceptor activation and damage by pulsed E-Fields. - art. no. 621904. Enabling Technologies and Design of Nonlethal Weapons. 2006; 6219:21904–21904.
38. Rogers WR, Merritt JH, Comeaux JA, Kuhnel CT, Moreland DF, Teltschik DG, Lucas JH, Murphy MR. Strength-duration curve for an electrically excitable tissue extended down to near 1 nanosecond. Ieee Transactions on Plasma Science. 2004; 32:1587–1599.
39. Nesin V, Pakhomov AG. Inhibition of voltage-gated Na(+) current by nanosecond pulsed electric field (nsPEF) is not mediated by Na(+) influx or Ca(2+) signaling. Bioelectromagnetics. 2012; 33:443–451. [PubMed: 22234846]
40. Semenov I, Zemlin C, Pakhomova ON, Xiao S, Pakhomov AG. Diffuse, non-polar electropermeabilization and reduced propidium uptake distinguish the effect of nanosecond electric pulses. Biochim Biophys Acta. 2015; 1848:2118–2125. [PubMed: 26112464]
41. Novickij, V., Pakhomova, ON., Saulis, G., Pakhomov, AG. Electric Field Dosimetry for Electroporation of Adherent Cells on Indium Tin Oxide (ITO)-Coated Glass Coverslips; 1st World Congress on Electroporation and Pulsed Electric Fields in Biology, Medicine and Food & Environmental Technologies (WC 2015)Portorož; Slovenia. 2015. p. 86-87.
42. Semenov I, Xiao S, Pakhomova ON, Pakhomov AG. Recruitment of the intracellular Ca by ultrashort electric stimuli: The impact of pulse duration. Cell Calcium. 2013; 54:145–150. [PubMed: 23777980]
43. Pakhomova ON, Khorokhorina VA, Bowman AM, Rodaite-Riseviciene R, Saulis G, Xiao S, Pakhomov AG. Oxidative effects of nanosecond pulsed electric field exposure in cells and cell-free media. Arch Biochem Biophys. 2012; 527:55–64. [PubMed: 22910297]
44. Nuccitelli R, Lui K, Kreis M, Athos B, Nuccitelli P. Nanosecond pulsed electric field stimulation of reactive oxygen species in human pancreatic cancer cells is Ca(2+)-dependent. Biochem Biophys Res Commun. 2013; 435:580–585. [PubMed: 23680664]
45. Levine ZA, Vernier PT. Calcium and phosphatidylserine inhibit lipid electropore formation and reduce pore lifetime. J Membr Biol. 2012; 245:599–610. [PubMed: 22815071]
46. Levine ZA, Vernier PT. Life cycle of an electropore: field-dependent and field-independent steps in pore creation and annihilation. J Membr Biol. 2010; 236:27–36. [PubMed: 20623350]
47. Gianulis EC, Lee J, Jiang C, Xiao S, Ibey BL, Pakhomov AG. Electroporation of mammalian cells by nanosecond electric field oscillations and its inhibition by the electric field reversal. Sci Rep. 2015; 5:13818. [PubMed: 26348662]
48. Weaver JC, Vanbever R, Vaughan TE, Prausnitz MR. Heparin alters transdermal transport associated with electroporation. Biochem Biophys Res Commun. 1997; 234:637–640. [PubMed: 9175766]
49. Weaver JC. Electroporation: a general phenomenon for manipulating cells and tissues. J Cell Biochem. 1993; 51:426–435. [PubMed: 8496245]
50. Sozer EB, Levine ZA, Vernier PT. Quantitative Limits on Small Molecule Transport via the Electropermeome - Measuring and Modeling Single Nanosecond Perturbations. Sci Rep. 2017; 7:57. [PubMed: 28246401]

51. Pakhomov AG, Semenov I, Xiao S, Pakhomova ON, Gregory B, Schoenbach KH, Ullery JC, Beier HT, Rajulapati SR, Ibey BL. Cancellation of cellular responses to nanoelectroporation by reversing the stimulus polarity. Cell Mol Life Sci. 2014; 71:4431–4441. [PubMed: 24748074]

52. Andre FM, Rassokhin MA, Bowman AM, Pakhomov AG. Gadolinium blocks membrane permeabilization induced by nanosecond electric pulses and reduces cell death. Bioelectrochemistry. 2010; 79:95–100. [PubMed: 20097138]

Highlights

- neurons were stimulated and electroporated by ultra-short 200-ns electric stimuli
- electroporation caused loss of resting membrane potential within < 1 ms
- recovery to the resting membrane potential took tens of seconds
- stimulation thresholds were the same or higher than electroporation thresholds

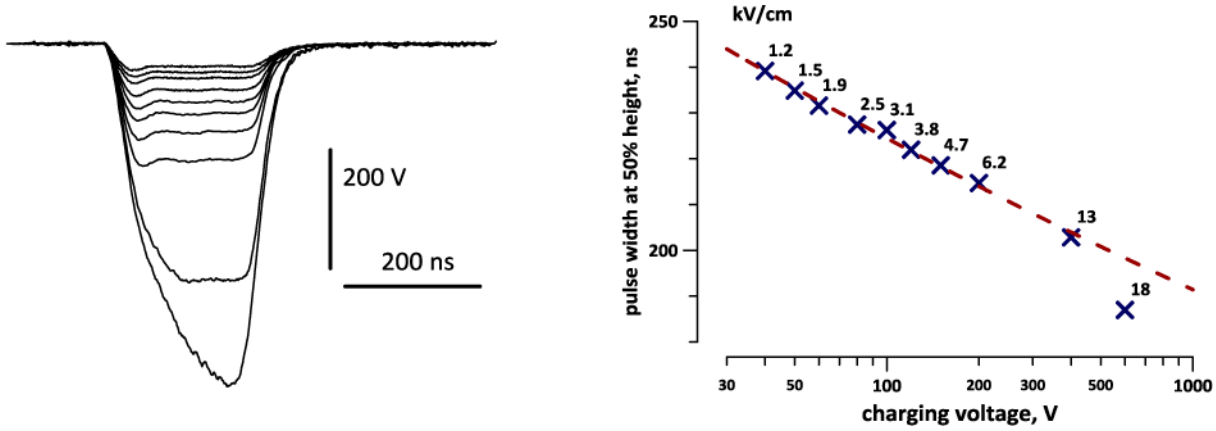

Fig. 1.

Traces of nanosecond pulses at different charging voltages (A) and the respective pulse width and the electric field (kV/cm) at the location of the stimulated neuron (B). The pulses were produced by charging the generator to 40, 50, 60, 80, 100, 120, 150, 200, 400, and 600 V. The amplitude of the pulse at the plateau (40–400V) is approximately the same as the charging voltage. The pulse width was measured at 50% of the plateau or of the peak (600 V). The inset illustrates the position of a stimulated neuron between two electrodes.

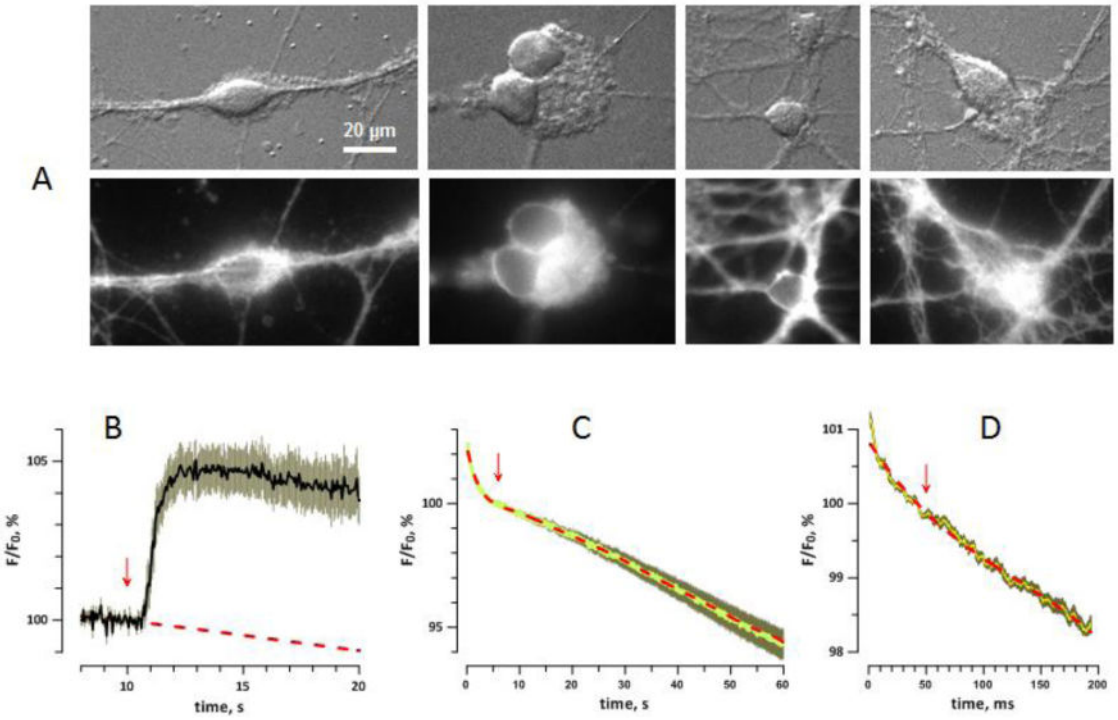

Fig. 2.

Imaging of the membrane potential with FluoVolt dye. A: Representative differential interference contrast (top) and fluorescence (bottom) images of dye-loaded neurons. Calibration bar applies to all panels. B: OMP change in response to bath perfusion by high-K^+ solution (arrow); mean +/− s.e., n=6. The dashed line is a linear fit for the region prior to the perfusion onset. Depolarization caused increase of the dye emission by about 5%. C: Average change of dye emission during a 1-min time-lapse imaging at 20 frames/s. The central bright line is the mean for 32 cells; the darker contour is the s.e. for each of 1200 points. The dashed line (red) is the best fit using a 9^{th} degree polynomial function. The region immediately before “sham stimulation” (0 V, arrow) was taken as 100%; see text for more details. D: Change of dye emission during 200 ms of imaging at 2325.6 frames/s, averaged for 21 cells. Designations are the same as in C; the best fit is by 4^{th} degree polynomial.

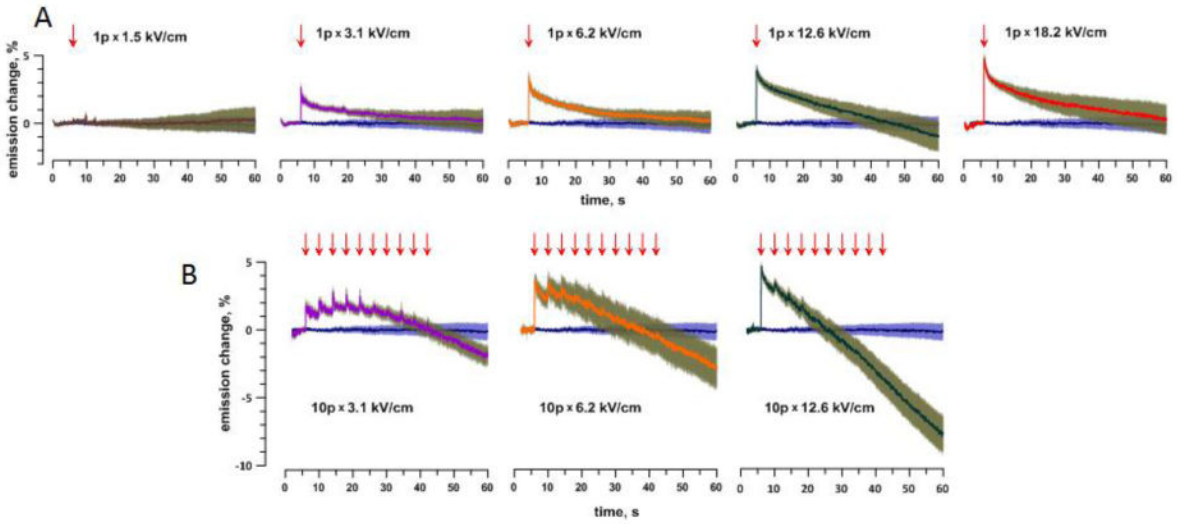

Fig. 3.

Persistent OMP depolarization in response to a single (A) or multiple (B) nsPEF at different amplitudes. Each panel shows the time course of FluoVolt emission change (%, mean +/− s.e., n=9–32) following the application of a single pulse (“1p”, arrow) or 10 pulses (“10p”) with 4-s intervals. The pulse amplitude (kV/cm) is in the legend. For comparison, each panel also includes the mean+/− s.e. data for a control group (stimulated at 0 kV/cm). All data were corrected for bleaching by subtracting the best fit curve from Fig. 2C. Note that the decrease of emission below the control value (“hyperpolarization”) is an artifact from enhanced dye bleaching in cells severely damaged by nsPEF. See text for more details.

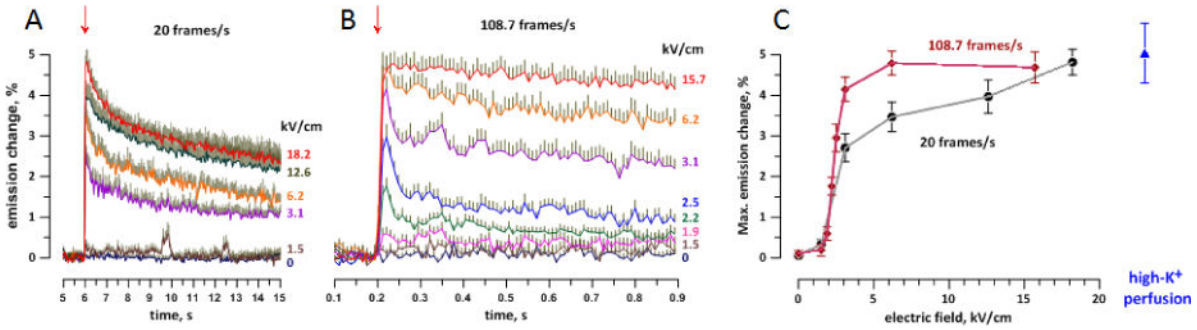

Fig. 4.

The early phase of nsPEF-induced OMP depolarization at different time scales (A and B) and the peak depolarization response versus the pulse amplitude (C). A: The same data as in Fig. 3, but plotted together and on a faster time scale. B: Data from an independent series of experiments, with faster imaging (108.7 frames/s, n=14–34). For clarity, error bars are shown in one direction only. Arrows show the time when nsPEF was delivered. The pulse amplitude (kV/cm) is in legends to the right of the plots. C: peak amplitude of depolarization, as measured from panels A and B, as compared with the response to depolarization by a high-K^+ solution (from Fig. 2B).

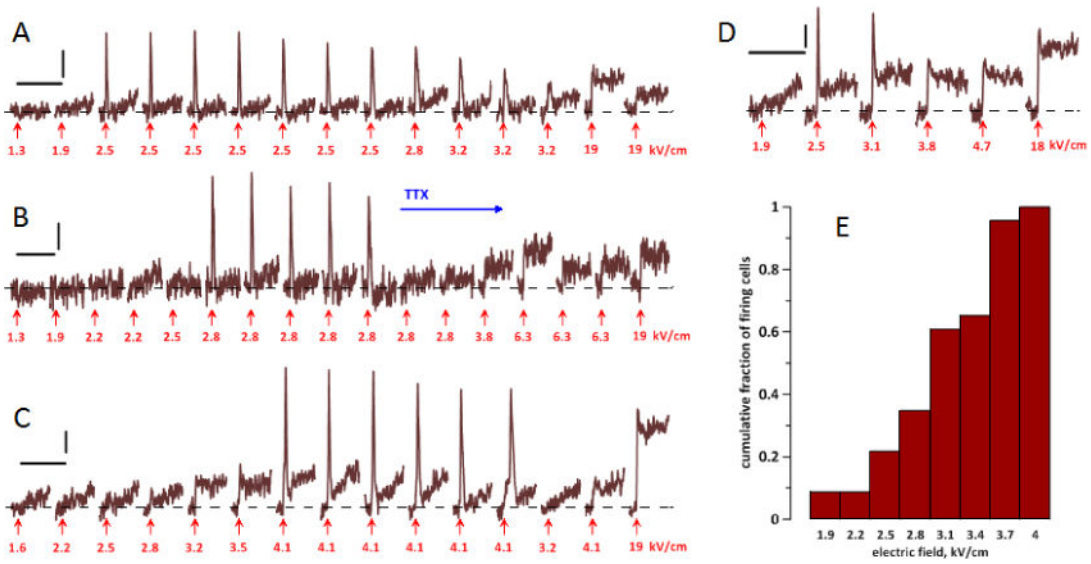

Fig. 5.

The induction of action potentials (APs) by nsPEF in four representative neurons (A–D) and a cumulative histogram of AP thresholds (E). A–D: Each neuron was subjected to multiple OMP recording and stimulation trials. Each trial lasted 193 ms (450 frames), with a single nsPEF applied at 50 ms (arrow); the trials are presented in the sequence they were performed (left to right). The interval between trials was always 1 min. Calibration bars are 200 ms and 1% emission change. The amplitude of each nsPEF is in the legend (kV/cm). APs appear as sharp peaks shortly after nsPEF; electroporation is manifested by the lack of MP return to the base level (dashed line). For noise reduction, all traces were smoothed with a “running average” filter over 9 sequential datapoints. In B, tetrodotoxin (TTX, 2 μM) was added to the bath when indicated. See text for more details. E: The cumulative fraction of cells firing AP at a certain stimulus amplitude (kV/cm), out of all cells which fired AP (n=23). The histogram includes cells both in normal and 0 Ca^{2+} Tyrode solution.

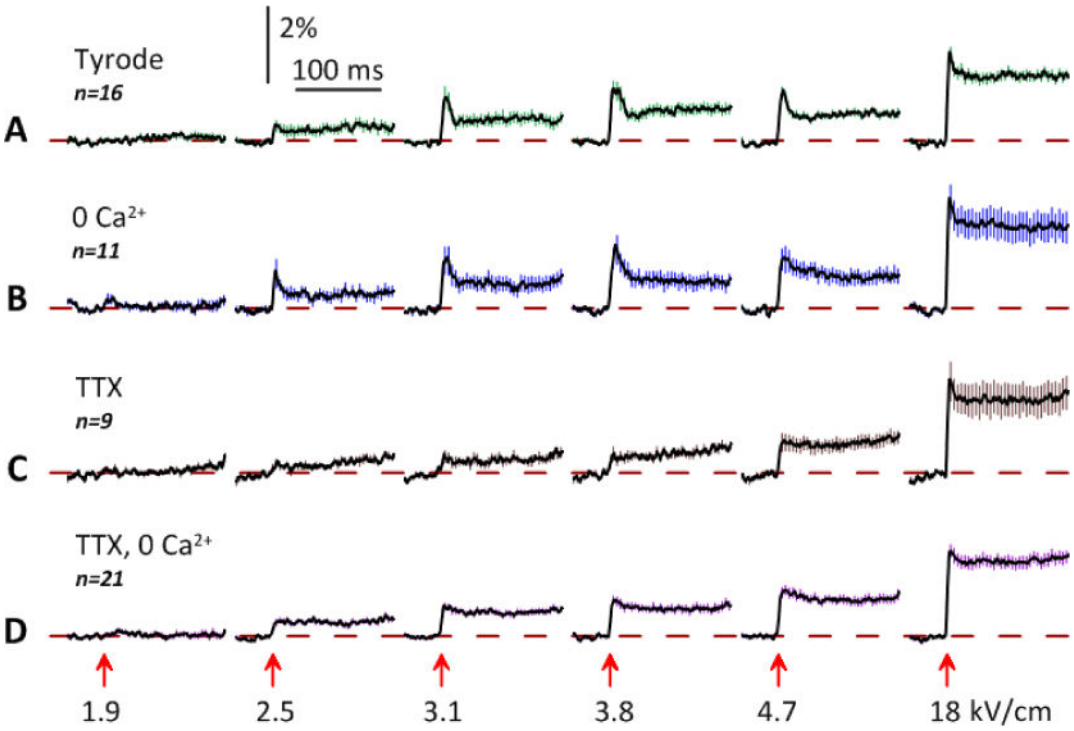

Fig. 6.

Contribution of VGSC and VGCC to the OMP change in response to nsPEF of increasing amplitude. Experiments were performed in: (A) standard Tyrode solution; (B) Tyrode solution composed without $CaCl_2$; (C) Tyrode solution with 4 μM tetrodotoxin (TTX); and (D) both without $CaCl_2$ and with 4 μM TTX. Each experiment included six OMP recording trials (193 ms, 450 frames each), with a stimulus of indicated amplitude (kV/cm) applied at 50 ms (arrow). The interval between trials was always 1 min. Shown are the mean traces +/− s.e. (for clarity, error bars are drawn for each 10^{th} datapoint only). Note the inhibition of the early depolarization peak by TTX and somewhat larger depolarization response in the 0 Ca^{2+} solution. See text for more details.

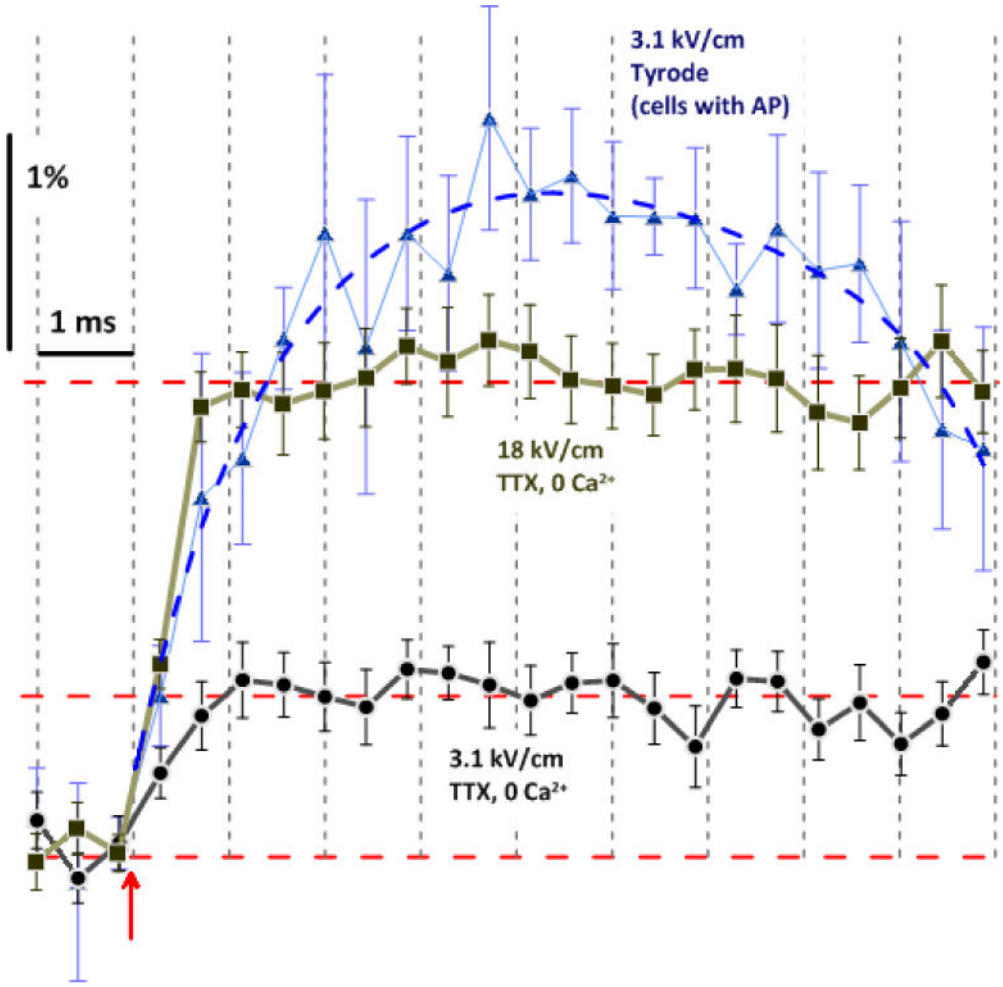

Fig. 7.

High-resolution time dynamics of depolarization and AP generation in response to nsPEF. All data are from respective trials in Fig. 6, plotted on a faster time scale and without "running average" filtering. For 3.1 kV/cm in standard Tyrode, we averaged the data only from those cells which fired AP (mean +/− s.e., n=5). The exposure duration for each frame was 0.43 ms; the datapoint position corresponds to the end of exposure. Note that, without the contribution of VG channels, the plateau level of depolarization (horizontal dashed lines) was reached already during the 2nd frame after nsPEF (arrow), both for 3.1 and 18 kV/cm. For 3.1 kV/cm, the difference between the data for normal Tyrode and TTX, 0 Ca^{2+} solution is the contribution of VG activation.